Soluble Solids and Simple Sugars Measurement in Intact Mango Using Near Infrared Spectroscopy

Stephen R. Delwiche[1,4], Weena Mekwatanakarn[2], and Chien Y. Wang[3]

Additional index words. *Magnifera indica*, mango, near-infrared, NIR interactance, soluble solids, nondestructive

Summary. **A rapid, reliable, and nondestructive method for quality evaluation of mango (*Magnifera indica*) fruit is important to the mango industry for international trade. The objective of this study was to determine the potential of near-infrared (NIR) spectroscopy to predict soluble solids content (SSC) and individual and combined concentrations of sucrose, glucose, and fructose nondestructively in mango. Mature mangoes at two different temperatures (15 °C and 20 °C) were measured by NIR interactance (750–1088 nm wavelength region analyzed) over an 11-day period, starting when the fruit were underripe and extending to a few days past optimal ripeness. Partial least squares regression was used to develop models for SSC, individual sugar concentration, and the sum of the concentrations of the three sugars. Such analyses yielded calibration equations with R^2 = 0.77 to 0.88 (SSC), 0.75 (sucrose), 0.67 (glucose), 0.70 (fructose), and 0.82 (sum); standard error of calibration = 0.56 to 0.90 (SSC), 10.0 (sucrose), 0.9 (glucose), 4.5 (fructose), and 10.4 (sum); and standard error of cross-validation = 0.93 to 1.10 (SSC), 15.6 (sucrose), 1.4 (glucose), 6.9 (fructose), and 16.8 (sum). When the SSC calibration was applied to a separate validation set, the standard error of performance ranged from 0.94% to 1.72%. These results suggest that for assessment of mango ripeness, NIR SSC calibrations are superior to the NIR calibrations for any of the individual sugars. This nondestructive technology can be used in the screening and grading of mangoes and in quality evaluation at wholesale and retail levels.**

The United States imports nearly all of the mangoes that its population consumes, estimated in value for 2006 (the latest available year) at $226 million (U.S. Department of Agriculture, 2007). Because sources are nondomestic (with Mexico, Haiti, and other central and South American countries, and recently, India, as prime suppliers), transport, quarantine, and pest treatment procedures necessitate that U.S.-consumed mangoes be harvested in a mature, but quite underripe state, weeks in advance of an optimal eating condition. Such long postharvest periods lead to decay and a large variation in the ripening times for individual fruit. Elsewhere, in places where mangoes are grown and consumed locally, eating quality and hence, fruit value, could also be enhanced through better quality assessment. Consumer choice of buying fresh fruit is becoming increasingly based on internal qualities, as opposed to merely appearance. In the past, external skin color, fruit size and shape, freedom from defects and abrasion, and the absence of decay were the most common quality determinants (Paull and Chen, 2004). The development of a rapid, reliable, nondestructive method for quality evaluation of mangoes is very important and critical to the mango industry and international trade. Sweetness is one of the most important factors that determine mango eating quality, particularly during ripening. Soluble solids content (SSC) and, to a smaller extent, sucrose, glucose, and fructose are the typical quality attributes for assessing mango sweetness and have shown usefulness in determining physiological changes during the ripening stage (Hatton et al., 1965, Kanes et al., 1982, Paull and Chen, 2004).

Although the exact relationships that would explain the changes in concentration of reducing (glucose and fructose) and nonreducing (sucrose) sugars during ripening are not agreed upon, it is generally accepted that sucrose accumulation occurs during this period, although only partially from the breakdown of starch (Castrillo et al., 1992). Therefore, sucrose concentration, and perhaps that of one or more of the reducing sugars, could be used, along with SSC, as an indicator of ripeness. However, determination of these constituents requires destructive methodology and, in the case of the sugars, expensive and labor-intensive equipment. Near-infrared (NIR) spectroscopy, which is a nondestructive method for fruit quality evaluation, has become a very popular technique and has been used to evaluate the internal quality of many fruit such as apple (*Malus ×domestica*; Lammertyn et al., 1998; Park et al., 2003, Zou et al., 2007), mandarin (*Citrus reticulata*; Guthrie et al., 2005; Kawano et al., 1993; McGlone et al., 2003), peach (*Prunus persica*;

We thank Mrs. Hilarine Repace, Produce Quality and Safety Laboratory, USDA-ARS, Beltsville, MD, for laboratory assistance.

The use or mention of any commercial product does not imply any endorsement of that product or any better suitability than other similar products by the authors or the U.S. Department of Agriculture.

[1]U.S. Department of Agriculture, Agricultural Research Service, Beltsville Agricultural Research Center, Food Safety Laboratory, Beltsville, MD 20705-2350

[2]Department of Horticulture, Faculty of Agriculture, Ubon Ratchathani University, Ubon Ratchathani, 34190, Thailand

[3]U.S. Department of Agriculture-Agricultural Research Service, Beltsville Agricultural Research Center, Produce Quality and Safety Laboratory, Beltsville, MD 20705

[4]Corresponding author. E-mail: Stephen.Delwiche@ars.usda.gov.

Units

To convert U.S. to SI, multiply by	U.S unit	SI unit	To convert SI to U.S., multiply by
0.3048	ft	m	3.2808
25.4	inch(es)	mm	0.0394
1	micron	µm	1
28.3495	oz	g	0.0353
28,350	oz	mg	3.5274×10^{-5}
0.001	ppm	$mg \cdot g^{-1}$	1000
(°F – 32) ÷ 1.8	°F	°C	(1.8 × °C) + 32

Kawano et al., 1992, 1995; Ying et al., 2005), kiwi (*Actinidia chinensis*; McGlone and Kawano, 1998), apricot (*Prunus armeniaca*; Manley et al., 2007), and mango (Guthrie and Walsh, 1997; Mahayothee et al., 2004; Saranwong et al., 2001, 2003, 2004; Schmilovitch et al., 2000). A more limited body of work exists for NIR analysis of individual sugars in juice (Li et al., 1996; Rodriguez-Saona et al., 2001), and none for such analysis of intact mango. Therefore, the objective of this study was to assess the potential of using NIR spectroscopy in measuring SSC in conjunction with concentrations of fructose, glucose, and sucrose in whole mango fruit.

Materials and methods

Plant material. Six cartons from one lot of Mexican-grown (Chiapas state) mango fruit (cv. Ataulfo) were purchased from an Asian market in Maryland and transported to the USDA laboratory in Beltsville, Maryland. Before import, the mangoes were subjected to hot water treatment in accordance with USDA Animal and Plant Health Inspection Service regulation for preventative control of the mediterranean fruit fly (*Ceratitis capitata*) and the mexican fruit fly (*Anastrepha ludens*). Standard treatment specifies an immersion temperature and time of 46 °C and 65 to 70 min, respectively (USDA, 2006). Three decayed fruit were immediately discarded, leaving a total of 93 mangoes, all preclimacteric, for analysis. Thirteen mangoes were individually weighed and scanned by NIR on the next day after market, and the remaining 80 fruit were weighed and scanned in groups of 20 on days 4, 5, 7, and 11 postmarket, with half the mangoes within each group stored at 15 °C and the other half at 20 °C. Variation in storage time and temperature was instituted for the purpose of ensuring all stages of ripeness, from a firm-textured, greenish, smooth-skinned underripe state to a soft-textured, bright yellowish, wrinkled skin overripe, nondecayed state (Miller et al., 1986). Fruit at the higher and lower storage temperatures were allowed to warm to ambient conditions (24 ± 1 °C) for 1 and 2 h, respectively, before scanning.

NIR measurement. NIR spectra (400–1098 nm, 2-nm increment) were collected using an NIR spectrometer equipped with a bifurcated fiber optic probe (model 6500 with Interactance Probe; Foss NIR Systems, Silver Spring, MD). Contained within the stainless steel probe housing are an annular region (8.9 mm radius, 0.5 mm thickness) that conveys monochromatic light from the spectrometer to the fruit, and an inner core (7.6 mm) that conveys the reflected light to the spectrometer's silicon detector (amplifier gain = 10×). Each mango, with its stem-calyx axis oriented horizontally, was positioned atop the upwardly pointing probe, with the flattest region of the fruit in contact with the probe (Fig. 1). A spectrum was collected on each lateral face of the mango, thus producing two spectra per fruit. A reference measurement of a Teflon cylinder with cylindrical well (of diameter equaling the diameter of the probe) was made before measurement of every fruit. To shield the fruit from ambient light, the probe was confined in an aluminum frame enclosure draped with black cloth. Additionally, separate reflectance spectra were collected of the amorphous structures of D-(−)-fructose, D-(+)-glucose, and sucrose. The amorphous states were prepared by dissolving each sugar in distilled water, dispersing the solution in a matrix of powdered sodium sulfate (≈1 solution:5 matrix, w/w), and then drying to an amorphous state. Sodium sulfate was used as a scattering reflectance background because of its low and nonspecific absorption characteristics and because it prevented the sugars from recrystalizing upon drying.

Determination of quality parameters destructively. The juice from flesh (≈5 g) directly underlying the probe contact point was extracted by a handheld garlic press. A digital refractometer with readout precision of 0.1% (model PR101; ATAGO, Tokyo) was used to measure the SSC (in units of percent, w/w) of the juice. Additional tissue specimens of 15 to 20 g were cut from these regions in 27 of the 93 mangoes. The number for this subset arose from a random selection of three of 13 fruit on day 1, and three of 10 fruit from each of the eight subsequent day-temperature groups. These specimens were frozen for later sugars analysis by gas chromatography.

Analysis of sugars. Two grams of mango fruit tissue were homogenized with a Polytron homogenizer (Brinkmann Instruments, Westbury, NY) in imidazole buffer (20 mM, pH

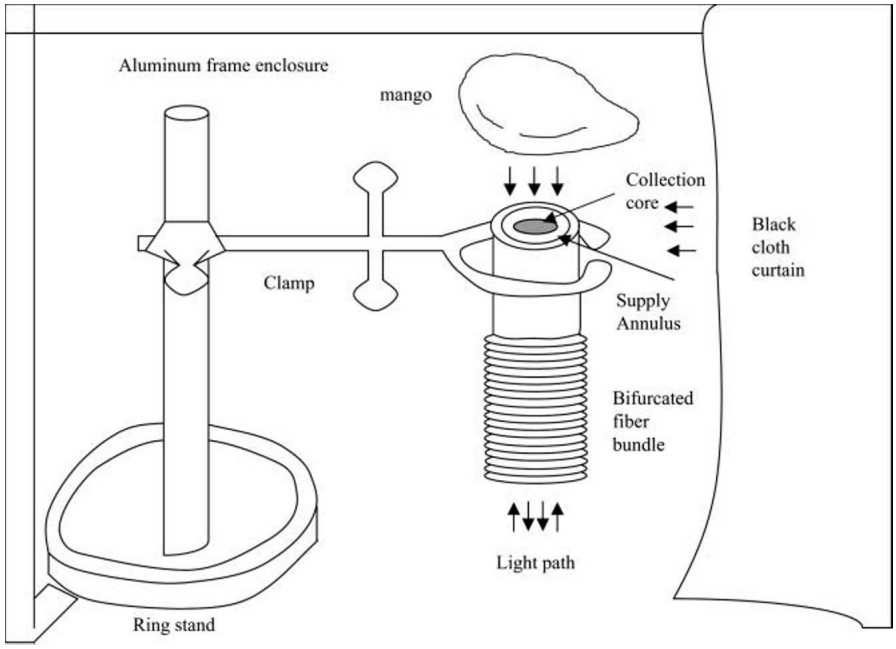

Fig. 1. Schematic presentation of NIR spectral acquisition system for nondestructive evaluation of sugars in intact mango fruit.

7.0). The extracts were centrifuged and the supernatants were dried in vacuo in derivatizing vials. Procedures described by Li and Schuhmann (1980) were modified for the derivatization of sugars. A known amount of β-phenyl-D-glucopyranoside was included in all samples as an internal standard. One milliliter of Trisil reagent (Pierce, Rockford, IL) was mixed vigorously with each sample and then heated at 75 °C for 30 min. After silylation, 1 μL of each derivatized sample was injected into a gas chromatograph (model 5890; Hewlett Packard, Palo Alto, CA) equipped with a flame ionization detector and a 25-m crosslinked methyl silicon gum capillary column (0.2-mm ID, 0.33-μm film thickness, helium carrier gas). Temperatures were as follows: injector 250 °C, detector 275 °C, and the column temperature was programmed to increase from 100 to 250 °C at 10 °C min^{-1}, and was then held constant at 250 °C for 23 min. The sugars, fructose, glucose, and sucrose, were quantified, in single analyses, by comparison with derivatized standards, and are reported in units of mass concentration (e.g., milligrams sugar per gram of fresh weight).

Spectral analysis. The Unscrambler multivariate analysis software program (version 9.1; CAMO, Oslo, Norway) was used for partial least squares (PLS) regression calibration development and validation. Because the penetration depth of radiation in the mango is less than 10 mm [at λ = 900 nm (Saranwong et al., 2001)], each side's spectrum was treated as a separate sample, with accompanying chemical assays, during NIR calibration development. Spectral pretreatments of second derivative [Savitzky-Golay, second order polynomial with 11-point, or 20-nm, convolution window (Savitzky and Golay, 1964)] were applied to reduce spectral variation caused by nonchemical variation, such as fruit shape. This window size was chosen based on preliminary calibration trials (data not shown), with narrower windows producing erratic calibration performance that varied with the spectra selected for calibration, and wider windows degrading performance through a loss of spectral features.

Because of the relatively large number of spectra (n = 186) available for SSC calibration development, separate calibration and validation sets were used for this analyte. Three-quarters of the mangoes were selected at random for use in calibration, and the remaining one-quarter was reserved for model validation. The number of PLS factors for each saved calibration equation was that associated with the minimum in standard error of cross-validation, using cross-validation structure of a leave-one-fruit-out (= 2-spectra-out) rotation. Modeling of the simple sugars was performed similarly, with the exception that the small number of fruit (27 fruit, 54 spectra) analyzed by the reference chemical method precluded the use of a separate validation set.

Results and discussion

Descriptive statistics of SSC and the sugars are presented in Table 1. The mean and standard deviation of fruit mass at the time of scanning were 273.7 and 21.5 g, respectively. In agreement with Castrillo et al. (1992), sucrose, with a mean concentration of 103.4 $mg \cdot g^{-1}$ was more abundant than fructose (21.9 $mg \cdot g^{-1}$) or glucose (3.1 $mg \cdot g^{-1}$). Fructose concentration increased slightly (1.7 and 1.6 $mg \cdot g^{-1} \cdot d^{-1}$ at 15 °C and 20 °C, respectively), though significantly ($P < 0.01$) during the storage period for both storage temperatures, as did the sucrose concentration of samples stored at 15 °C (5.5 $mg \cdot g^{-1} \cdot d^{-1}$). In contrast, glucose concentration decreased during this period (–0.5 and –0.4 $mg \cdot g^{-1} \cdot d^{-1}$ at 15 °C and 20 °C, respectively, $P < 0.01$).

PLS calibration performance for SSC is summarized in Table 2. Compared with initial calibrations involving the entire (400–1098 nm) wavelength region, truncation to 750 to 1098 nm was found to enhance performance (results not shown), such that the findings reported herein reflect the truncated wavelength region. Similar improvement with wavelength truncation was noted for apples (Park et al., 2003) and mandarin fruit (McGlone et al., 2003). Model improvement through removal of the visible region wavelengths is consistent with an imperfect correlation between sweetness and skin color.

With all calibration set mangoes included (n = 138 spectra) in the regression model for SSC, the coefficient of determination (R^2) was 0.77, and the standard error of calibration (SEC) and standard error of cross-validation (SECV) were 0.90% and 1.10%, respectively. The optimal number of factors was six. The corresponding standard error of performance (SEP), as determined from the application of the calibration equation to the validation set (n = 48 spectra), was 1.43%, with a bias of 0.21%. Two validation samples, which corresponded to the smallest and largest SSC values by reference analysis, produced residual values that were more than three times the standard error. With removal of the most outlying and second most outlying samples, the SEP dropped to 1.15% and 1.02%, respectively. The ratio of the standard deviation of the reduced validation set to the SEP [i.e., the RPD (Williams, 2001)] was 2.0, which may be of use in screening. A plot of predicted versus measured readings of SSC for this second case is shown in Fig. 2. Removal of day 1

Table 1. Descriptive statistics of the measured properties in the study, which examined the ability of NIR spectroscopy to measure the SSC and the individual and combined concentrations of fructose, glucose, and sucrose in intact mangoes.

Analyte	Samples (no.)	Range	Mean	SD	Units[z]
SSC, calibration set	138	11.7–23.1	17.53	1.87	%
SSC, validation set	48	12.0–26.9[y]	17.43	2.57	%
Fructose	54	9.3–41.0	21.87	8.13	$mg \cdot g^{-1}$
Glucose	54	0.3–5.9	3.14	1.62	$mg \cdot g^{-1}$
Sucrose	54	63.5–155.35	103.36	20.07	$mg \cdot g^{-1}$
Sum of three sugars	54	76.7–181.6	128.37	24.38	$mg \cdot g^{-1}$

[z]1 $mg \cdot g^{-1}$ = 1000 ppm.

[y]Removal of a validation sample with the largest residual (i.e., the difference between the value predicted by NIR and that determined by the reference procedure) resulted in a range, mean, and SD of 12.0% to 22.7%, 17.23%, and 2.18%, respectively. Further removal of a validation sample with the second largest residual resulted in corresponding values of 13.6% to 22.7%, 17.34%, and 2.06%, respectively.

Table 2. Summary of the PLS regression statistics for the NIR-based models of SSC in intact mango fruit.

Description or condition of samples	PLS factors (no.)[z]	Calibration set				Validation set		
		Samples (no.)	R^{2y}	SEC (% SSC)[x]	SECV (% SSC)[w]	*N*	SEP (% SSC)[v]	Bias (% SSC)[u]
All	6	138	0.77	0.90	1.10	48	1.43	0.21
(less 1 validation set spectrum)						47	1.15	0.33
(less 2 validation set spectra)						46	1.02	0.25
All, excluding day 1	6	120	0.82	0.75	0.93	40	1.53	0.18
(less 1 validation set spectrum)						39	1.11	0.35
Stored at 15 °C (59.0 °F)	6	60	0.88	0.56	0.93	20	0.94	0.11
Stored at 20 °C (68.0 °F)	6	60	0.87	0.68	1.09	20	1.72	0.01
(less 1 validation set spectrum)						19	1.32	0.26

[z]PLS factors = number of partial least squares factors used in calibration equation.
[y]R^2 = coefficient of determination.
[x]SEC = standard error of calibration.
[w]SECV = bias-corrected standard error of cross-validation.
[v]SEP = standard error of performance.
[u]Bias = difference between mean of the NIR-predicted values and the mean of the reference method values.

samples from the original calibration and validation sets (because these mangoes were shielded from room light differently than those of subsequent days) resulted in a slight improvement in calibration performance (n_{cal} = 120, R^2 = 0.82, SECV = 0.93%; n_{val} = 39, SEP = 1.11%).

The level of SSC modeling error in the present study is intermediate with respect to other published work on mangoes [SEP = 0.46% (Saranwong et al., 2001); SEP = 1.4% to 1.9% (Mahayothee et al., 2004)]; however, direct comparison with other research studies is difficult owing to differences in the source, the range and distribution of SSC, the spectral measurement procedure, and the handling of outliers. By way of example, this difficulty is shown using subsets of samples from the present study (Table 2). When just the samples from the 15 °C storage temperature were used, the SECV (n = 60) and SEP (n = 20) were 0.93% and 0.94%, respectively. These values are contrasted with the corresponding values of 1.09% and 1.72% for the samples stored at 20 °C.

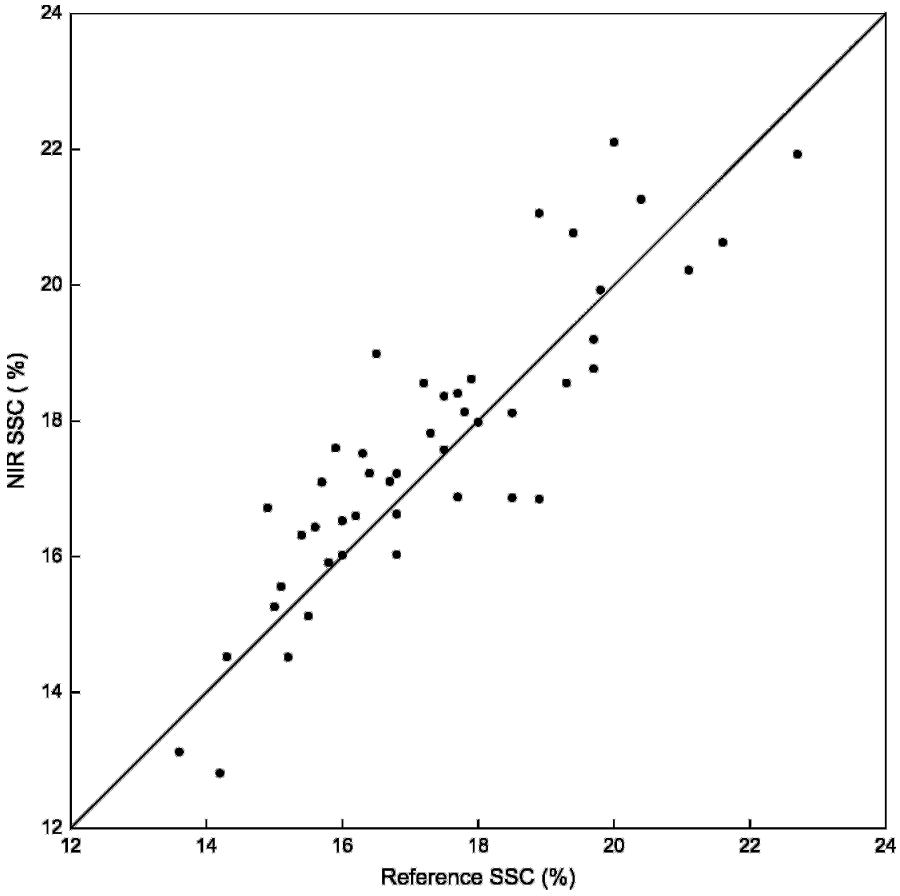

Fig. 2. Scatter plot between actual and NIR-predicted values for SSC of a validation set (n = 46), which consisted of mangoes stored at two temperatures [15 and 20 °C (59.0 and 68.0 °F)], and scanned on five occasions (days 1, 4, 5, 7, and 11, postmarket). SEP = standard error of performance; bias = difference between mean of the NIR-predicted values and the mean of the reference method values; n = number of samples.

Modeling performance of the individual sugars and their sum are summarized in Table 3. The coefficient of determination (R^2) ranged from 0.67 (glucose) to 0.82 (sum of fructose, glucose, and sucrose). With removal of one fruit as an outlier in the glucose calibration, the R^2 increased to 0.81. Generally, SSC calibrations were superior to the individual sugar calibrations (RPD = 1.2, 1.1, 1.3, and 1.5 for fructose, glucose, sucrose, and sum of the three sugars, respectively). Scatter plots of NIR versus reference values for the individual sugar models and the sum of all three sugars model are depicted in Fig. 3. The relatively poor performances of the individual sugar calibrations are attributed to the combination of their low concentration, difficulty in precise chemical measurement, and their spectral similarity.

Table 3. Summary of the PLS regression statistics for the NIR-based models of the individual and combined concentrations of fructose, glucose, and sucrose in intact mango fruit.

Sugar	Samples (no.)	PLS factors (no.)[z]	R^{2y}	SEC (mg·g^{-1})[x]	SECV (mg·g^{-1})[w]	Bias (mg·g^{-1})[v]
Fructose	54	6	0.70	4.48	6.91	0.01
Glucose	54	6	0.67	0.93	1.44	–0.06
(less one outlier pair)	52	6	0.81	0.69	1.25	0.07
Sucrose	54	4	0.75	10.05	15.59	1.88
Sum of three sugars	54	6	0.82	10.35	16.80	–0.43

[z]PLS factors = number of partial least squares factors used in calibration equation.
[y]R^2 = coefficient of determination.
[x]SEC = standard error of calibration (1 mg·g^{-1} = 1000 ppm).
[w]SECV = bias-corrected standard error of cross-validation.
[v]Bias = difference between mean of the NIR-predicted values and the mean of the reference method values.

Compared with the other two sugars, sucrose produced better PLS performance for probable reasons of its greater abundance and higher correlation to SSC ($r_{SSC\ vs.\ sucrose}$ = 0.72, compared with $r_{SSC\ vs.\ glucose}$ = –0.03 and $r_{SSC\ vs.\ fructose}$ = 0.32). From the standpoint of NIR analysis, the relative abundance of sucrose is fortunate, considering that sucrose is the best indicator of sweetness in mango fruit (Saranwong et al., 2001). During fruit development, sucrose was found to accumulate the greatest amount of the carbon released from the breakdown of starch (Léchaudel et al., 2005). Additionally, the mango ripening stage brings on the increase in fructose and glucose and a reduction in titrable acidity (Selvaraj et al., 1989). However, these trends are not consistent in the literature, as exemplified by Selvaraj et al. (1989), who reported a lower concentration for sucrose than glucose or fructose, despite all three sugars increasing in concentration during ripening.

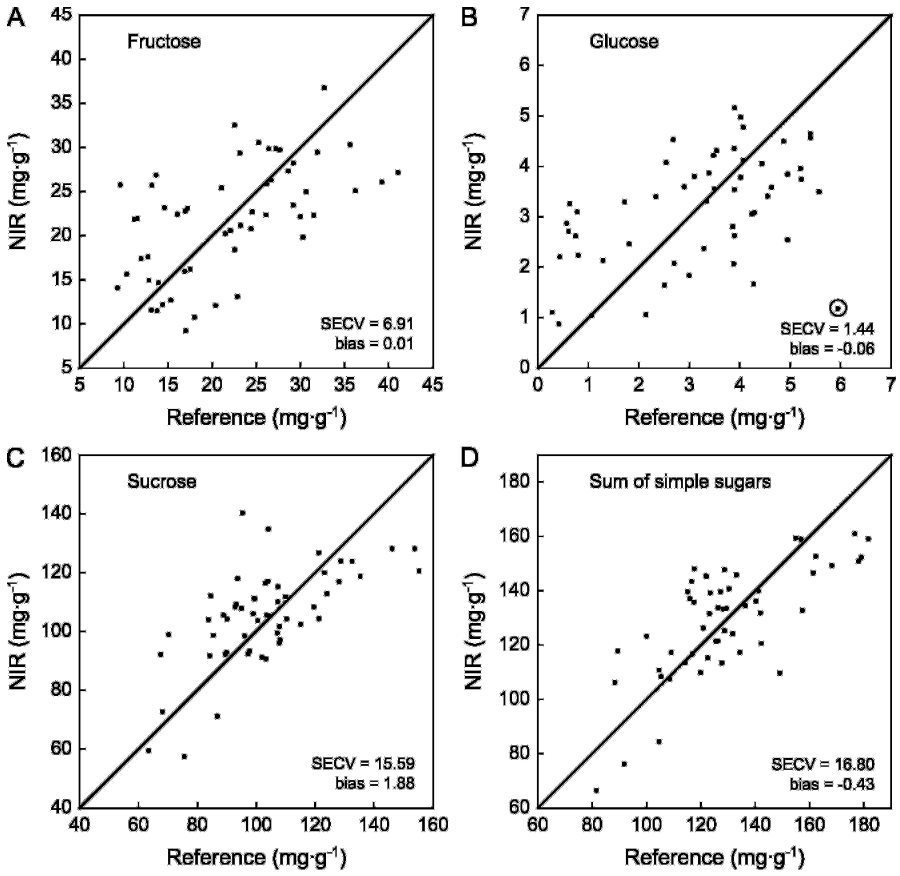

Fig. 3. Scatter plots between actual and NIR-predicted values for selected sugar concentrations (A = fructose, B = glucose, C = sucrose, and D = sum of the three) by cross-validation (n = 54) for mangoes stored at two temperatures [15 and 20 °C (59.0 and 68.0 °F)] and scanned on five occasions (days 1, 4, 5, 7, and 11, postmarket). The circled point in Graph B corresponds to the outlier that, along with its corresponding reading from the opposite side of the fruit, was removed for reanalysis of the partial least squares calibration, as reported in Table 3. SECV = bias-corrected standard error of cross-validation; bias = difference between mean of the NIR-predicted values and the mean of the reference method values (1 mg·g^{-1} = 1000 ppm).

The spectral differences among the sugars were very small. Complicating this is the fact that the sugar absorption bands [generally from the second and third overtones of oxygen-hydrogen (OH) stretches, and third and fourth overtones of carbon-hydrogen (CH) stretches] occur near strong water absorption regions. Furthermore, the sugars and temperature affect the degree of hydrogen bonding within the water molecules and hence the cluster arrangement of these molecules (Giangiacomo, 2006). According to Luck (1974), organic and inorganic solutes affect the spectral water absorption bands through alteration of the distribution of its hydrogen bands. Such changes affect absorption magnitude and frequency of vibration. The extent of the vibration or wavelength shift and the direction thereof, whether the shift is toward lower wavelengths (indicative of a disruption in the hydrogen bonding among the water molecules) or higher wavelengths (enhancement of water hydrogen bonding) is noted to depend on the concentration of the sugar (Giangiacomo, 2006). Low concentrations promote the disruption of water hydrogen bonding, whereas high concentrations produce the opposite effect. Spectral differences among the sugars are displayed by their first three PLS loadings in Fig. 4 (lower three graphs). Also shown are the second derivative spectra of the individual sugars in an aqueous medium (upper graph). For the first loading, the largest variation occurred in the 900- to 1000-nm region, largely attributed to water absorption. For this loading, SSC was the most different, although all four analytes demonstrated the same

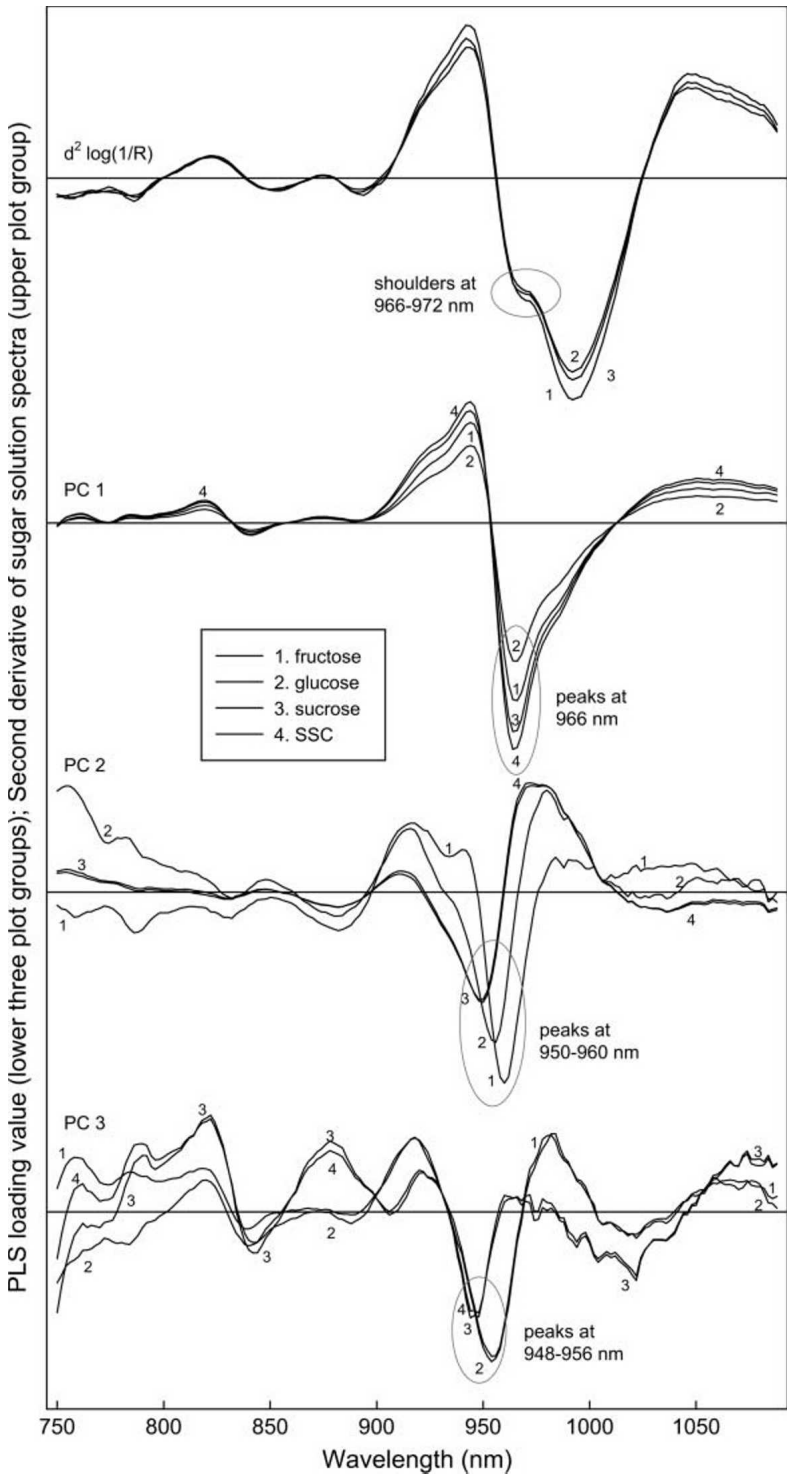

Fig. 4. Loadings of the first three factors of the PLS regression models for sugars (fructose, glucose, and sucrose) and SSC, and the second derivative (11-point Savitzky-Golay convolution, second order polynomial) of spectra of these pure sugars in a matrix of sodium sulfate. PC = principal component.

overall response. The region of greatest difference, near the downward peak at 966 nm, coincided with a shoulder in the second derivative at 966 to 972 nm, which also showed variation among the sugars. Compared with the first loading, the second loading demonstrated greater relative variation among the sugars, with fructose being the most different. Unlike the derivative and first loading plots, the second loading plots displayed a wavelength shift in peak absorption at 950 to 960 nm, with sucrose and SSC located near 950 nm and fructose and glucose located near 960 nm. These shifts are indicative of the unique role that each sugar has in the disruption of water structure. This pattern was also apparent in the third loading plots, with fructose and glucose behaving similarly in the 948- to 956-nm water band region, and sucrose and SSC shifted toward lower end of this region. Hence, sucrose appears to have a greater effect in disrupting water structure (i.e., structure-breaker effect) than fructose or glucose.

In conclusion, we find that when using NIR technology for assessing mango ripeness and quality, SSC, compared with the concentrations of the individual sugars (fructose, glucose, and sucrose), should continue to be the preferred constituent that is measured, followed by sucrose. The technique may be useful for segregating fruit by level of SSC at all stages between the packing house and the retail store.

Literature cited

Castrillo, M., N.J. Kruger, and F.R. Whatley. 1992. Sucrose metabolism in mango fruit during ripening. Plant Sci. 84:45–51.

Giangiacomo, R. 2006. Study of water-sugar interactions at increasing sugar concentration by NIR spectroscopy. Food Chem. 96:371–379.

Guthrie, J. and K. Walsh. 1997. Non-invasive assessment of pineapple and mango fruit quality using near infra-red spectroscopy. Austral. J. Expt. Agr. 37:253–263.

Guthrie, J., K. Walsh, and D. Reid. 2005. Assessment of internal quality attribute of mandarin fruit. 1. NIR calibration model development. Austral. J. Agr. Res. 56:405–416.

Hatton, T.T., W.F. Reeder, and C.W. Campbell. 1965. Ripening and storage of Florida mangos. U.S. Dept. Agr. Market Res. Rpt. 725.

Kanes, O., M. Boulet, and F. Costaigne. 1982. Effect of chilling injury on texture and fungal rot of mangoes (*Mangifera indica* L.). J. Food Sci. 47:992–995.

Kawano, S., H. Abe, and M. Iwamoto. 1995. Development of a calibration equation with temperature compensation for determining the Brix value in intact

peaches. J. Near Infrared Spectroscopy 3:211–218.

Kawano, S., T. Fujiwara, and M. Iwamoto. 1993. Nondestructive determination of sugar content in Satsuma mandarin using near infrared (NIR) transmittance. J. Jpn. Soc. Hort. Sci. 62:465–470.

Kawano, S., H. Watanabe, and M. Iwamoto. 1992. Determination of sugar content in intact peaches by near infrared spectroscopy with fiber optics in interactance mode. J. Jpn. Soc. Hort. Sci. 61:445–451.

Lammertyn, J., B. Nicolaï, K. Ooms, V. De Smedt, and J. De Baerdemacker. 1998. Non-destructive measurement of acidity, soluble solids, and firmness of Jonagold apples using NIR spectroscopy. Trans. Amer. Soc. Agr. Eng. 41:1089–1094.

Léchaudel, M., J. Joas, Y. Caro, M. Génard, and M. Jannoyer. 2005. Leaf-fruit ration and irrigation supply affect seasonal changes in minerals, organic acids and sugars of mango fruit. J. Sci. Food Agr. 85:251–260.

Li, W., P. Goovaerts, and M. Meurens. 1996. Quantitative analysis of individual sugars and acids in orange juices by near-infrared spectroscopy of dry extract. J. Agr. Food Chem. 44:2252–2259.

Li, B.W. and P.J. Schuhmann. 1980. Gas-liquid chromatographic analysis of sugars in ready-to-eat breakfast cereals. J. Food Sci. 45:138–141.

Luck, W.A.P. 1974. Infrared overtone region, p. 247–284. In: W.A.P. Luck (ed.). Structure of water and aqueous solutions. Verlag Chemie, Weinheim, Germany.

Mahayothee, B., W. Muhlbauer, S. Neihart, M. Leitenberger, and R. Carle. 2004. Non-destructive determination of maturity of Thai mangoes by near-infrared spectroscopy. Acta Hort. 645:581–588.

Manley, M., E. Joubert, L. Myburgh, E. Lotz, and M. Kidd. 2007. Prediction of soluble solids content and post-storage internal quality of Bulida apricots using near infrared spectroscopy. J. Near Infrared Spectroscopy 15:179–188.

McGlone, V.A., D.G. Fraser, R.B. Jordan, and R. Kunnemeyer. 2003. Internal quality assessment of mandarin fruit by vis/NIR spectroscopy. J. Near Infrared Spectroscopy 11:323–332.

McGlone, V.A. and S. Kawano. 1998. Firmness, dry matter and soluble solids assessment of postharvest kiwifruit by NIR spectroscopy. Postharvest Biol. Technol. 13:131–141.

Miller, W.R., D.H. Spalding, and P.W. Hale. 1986. Film wrapping mangos at advanced stages of post-harvest ripening. Trop. Sci. 26:9–17.

Park, B., J.A. Abbott, K.J. Lee, C.H. Choi, and K.H. Choi. 2003. Near-infrared diffuse reflectance for quantitative and qualitative measurement of soluble solids and firmness of Delicious and Gala apples. Trans. Amer. Soc. Agr. Eng. 46:1721–1731.

Paull, R.E. and C.C. Chen. 2004. Mango. In: K.C. Gross, C.Y. Wang, and M. Saltveit (eds.). The commercial storage of fruits, vegetables, and florist and nursery stocks. 21 Nov. 2007. <http://www.ba.ars.usda.gov/hb66/index.html>.

Rodriguez-Saona, L.E., F.S. Fry, M.A. McLaughlin, and E.M. Calvey. 2001. Rapid analysis of sugars in fruit juices by FT-NIR spectroscopy. Carbohydr. Res. 336:63–74.

Saranwong, S., J. Sornsrivichai, and S. Kawano. 2001. Improvement of PLS calibration for Brix value and dry matter of mango using information from MLR. J. Near Infrared Spectroscopy 9:287–295.

Saranwong, S., J. Sornsrivichai, and S. Kawano. 2003. Performance of a portable NIR instrument for Brix value determination of intact mango fruit. J. Near Infrared Spectroscopy 11:175–181.

Saranwong, S., J. Sornsrivichai, and S. Kawano. 2004. Prediction of ripe stage eating quality of mango fruit from its harvest quality measured nondestructively by near infrared spectroscopy. Postharvest Biol. Technol. 31:137–145.

Savitzky, A. and M.J.E. Golay. 1964. Smoothing and differentiation of data by simplified least squares procedures. Anal. Chem. 36:1627–1639.

Schmilovitch, Z., A. Mizrach, A. Hoffman, H. Egozi, and Y. Fuchs. 2000. Determination of mango physiological indices by near-infrared spectrometry. Postharvest Biol. Technol. 19:245–252.

Selvaraj, Y., R. Kumar, and D.K. Pal. 1989. Changes in sugars, organic acids, amino acids, lipid constituents and aroma characteristics of ripening mango (*Mangifera indica* L.) fruit. J. Food Sci. Technol. 26:308–313.

U.S. Department of Agriculture. 2006. Treatment Schedule T102: a hot water dip, p. 5-2-49. In: Treatment manual. USDA, Animal and Plant Health Inspection Service, Riverdale, MD.

U.S. Department of Agriculture. 2007. Miscellaneous agricultural statistics, p. XV-1 to XV-38. In: Agricultural statistics. USDA, National Agricultural Statistics Service, Washington, DC.

Williams, P.C. 2001. Implementation of near-infrared technology, p. 145–169. In: P. Williams and K. Norris (eds.). Near-infrared technology in the agricultural and food industries. Amer. Assn. Cereal Chemists, St. Paul, MN.

Ying, Y.B., Y.D. Liu, J.P. Wang, X.P. Fu, and Y.B. Li. 2005. Fourier transform near-infrared determination of soluble solids and available acid in intact peaches. Trans. Amer. Soc. Agr. Eng. 48:229–234.

Zou, X., Y. Li, and J. Zhao. 2007. Using genetic algorithm interval partial least squares selection of the optimal near infrared wavelength regions for determination of the soluble solids content of 'Fuji' apple. J. Near Infrared Spectroscopy 15:153–159.